J. Condensed Matter Nucl. Sci. 13 (2013) 543–553

Research Article

Forcing the Pd/^{1}H–^1H_2O System into a Nuclear Active State

Stanislaw Szpak and Frank Gordon*

SPAWAR Systems Center (Retired), San Diego, CA USA

Abstract

In cells employing cathodes prepared by the co-deposition process, the polarized Pd/D–D_2O system becomes nuclear active when the concentration of deuterium, expressed as D/Pd atomic ratio, is equal to or greater than one. In contrast, to activate the polarized Pd/H–H_2O system, action of an external magnetic field and modulation of cell current or both are required. Evidence for the nuclear active state in the Pd/H–H_2O system, namely deuterium production, particle emission and catastrophic thermal event, is presented. Extension of nuclear active state to the Pd^{1}H/^1H_2O system under the application of an external magnetic field and modulated cell current profile is discussed.
 ISSN 2227-3123

Keywords: Nuclear Active State, Electron capture

1. Introduction

The emission of soft X-rays [1] and production of tritium [2] led us to the conclusion that an electron capture by a deuteron might be one of the nuclear reactions generating the F–P effect in the polarized Pd/D–D_2O system. We reviewed the available empirical evidence and concluded that the proper course of action is to examine in detail the content and meaning of the electron capture reaction. While the essential goal of nuclear physics is to interpret the nature of nuclear forces, that of nuclear chemistry is to cast transmutation in terms used in chemical reactions [3]. It does not matter which methodology is employed, because the governing laws are the same. In what follows, the discussion is limited to chemical reasoning and terminology. The transition from chemical to physical terminology is by substituting negative binding energy, $-\epsilon$, for chemical potential, μ, i.e. $\mu(\mathrm{p}) = -\epsilon(\mathrm{p})$.

1.1. The content and meaning of the electron capture reaction

In the Landau and Lifshitz Treatise [4] we find a nuclear reaction, which may be symbolically written as $A_Z + \mathrm{e}^- \rightarrow A_{Z-1} + \nu$, where A_Z denotes a nucleus of atomic weight A and charge Z, e^- an electron and ν a neutrino. The neutrinos are not retained by matter and leave the body. Nuclear reaction of this type may be represented by equations

*E-mail: dr.frank.gordon@gmail.com

 ISSN 2227-3123

which correspond exactly to those employed in chemical reactions. Consequently, it is not difficult to write down the thermodynamic conditions for the reaction

$$e^- + p^+ \rightarrow n \tag{1}$$

to proceed, namely that the inequality $\mu(e^-) > \mu(n) - \mu(p^+)$ is positive.

Equation (1) as written is the usual representation of a chemical reaction. It provides only limited information, namely it is the statement of conservation of mass, energy and charge. Since the initial and final states are not specified, it simply means that the system consists of unbounded particles in the sense that there is a continuous range of possible energies. Since there are two partners, electrons and lattice interacting protons, energies of both must be considered, a conclusion neglected in the Widom–Larsen theory.

1.2. Protons in lattice

All protons located in the reaction volume interact with the Pd lattice to a various degree. The chemical potential of interacting protons, p_l^+, is of the form $\mu(p_l^+) = \mu(p^+) + u(r)$ where $u(r)$ denotes the energy of interaction. To evaluate the $u(r)$ function, we consider the relation $\mu(p) = -\epsilon(p)$, i.e. the chemical potential of a particle p is its negative binding energy. In this representation, the $u(r)$ term indicates that a part of the interacting site is incorporated into the proton itself, i.e. it represents the degree of an overlap which, in turn, determines whether or not the electron capture by proton can occur. For an electron capture by a proton to occur, the quantity $\mu(n) - \mu(p_l^+)$ must be positive. Since light water electrolysis alone does not produce a nuclear active state, it follows that $\mu(p_l^+)$, is greater than that of the neutron, $\mu(n)$, i.e. irrespective of its energy, the electron capture by proton cannot occur.

1.3. Sequence of events

The sequence of events leading to the initiation of the nuclear active state is shown in a diagram, Fig. 1.

Here, the events within the metal side of the interphase are: an exchange between the adsorbed and absorbed hydrogen, H_{ad}, H_{ab}, the transition from atomic to nuclear state that occurs when the hydrogen atom gives up an electron and becomes a proton, denoted $H_{ab} \rightarrow p^+$, followed by $p^+ \rightarrow p_l^+$, the latter identifies a proton interacting strongly with the Pd lattice with the formation of a metalic bond. When an external magnetic field, ψ, is applied, a new set of processes can be identified, viz weakening of the interaction, $p_l^+ \rightarrow p_*^+$, electron capture by proton, $e^- + p_*^+ \rightarrow n$, with

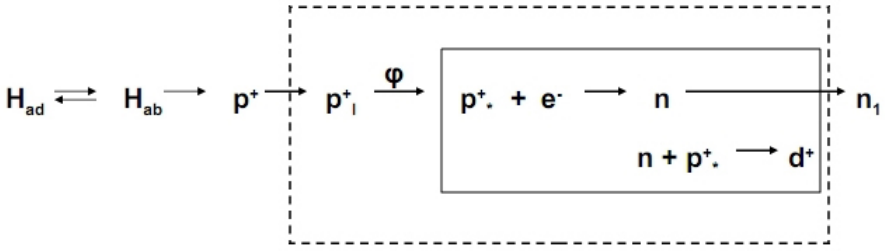

Figure 1. Schematic diagram showing events within the interphase. Enclosed by broken lines are processes affected by an external field; by solid line – coupled nuclear reactions.

neutrons either escaping, n_1, or reacting with proton to yield deuteron, $n + p_*^+ \rightarrow d^+$. At the beginning, the simplest, and the only reaction that yields neutrons in this system is the electron capture by proton.

2. Coupled Reaction

Under the action of an external magnetic field, the transition $p_l^* \rightarrow p_*^+$ takes place and, as indicated, reaction $e^- + p_*^+ \rightarrow n$ occurs. With the passage of time, the second, highly energetic reaction $n + p_*^+ \rightarrow d^+$, takes place to become the primary energy supplier for the first reaction. The reaction product, the deuteron, reacts with an electron, $e^- + d^+ \rightarrow 2n$. Here, we have a situation in which the first reaction is accelerated by its product via the energy supplied by the chemical change in the substance (here neutrons) which induces the first reaction. Restating: the first reaction is induced by the second and third reaction via the energy transfer. Such kinetics is referred to as induction kinetics [6].

3. Forcing into Nuclear Active State – Effect of Magnetic Field

The interaction of a magnetic field with electrochemical systems can be divided into three main areas: (i) magneto-hydrodynamic effects, i.e. those affecting mass transport via the reduction of the diffusion layer thickness, (ii) magneto-mechanical effects, i.e. those that involve the shape change of micro-globules as well as complex macro-molecules, Fig. 2, and (iii) non-specific interactions of electronic nature, i.e. those affecting dynamics of the highly concentrated hydrogen in the Pd lattice. These effects are attributed to forces generated by the gradients of magnetic energy density, i.e. by forces that arise from non-homogeneity of the paramagnetic entity and those associated with non-uniformity of the magnetic field.

The data presented in Fig. 3 show typical potential/time curve for the desorption of hydrogen from the electrode having structure shown in Fig. 2b, in absence and presence of an external magnetic field, curves a and b, respectively. Here, the electrode potential/time relation, $\Phi(t)$, shows, Fig. 3, that the time for the transition from transport to surface controlled desorption of hydrogen, segments AB and BC, is substantially shorter when an external magnetic field was applied. Such behavior indicates that magnetic field weakens the proton/Pd defect interaction, i.e. $\mu(p_l^+) > \mu(p_*^+)$.

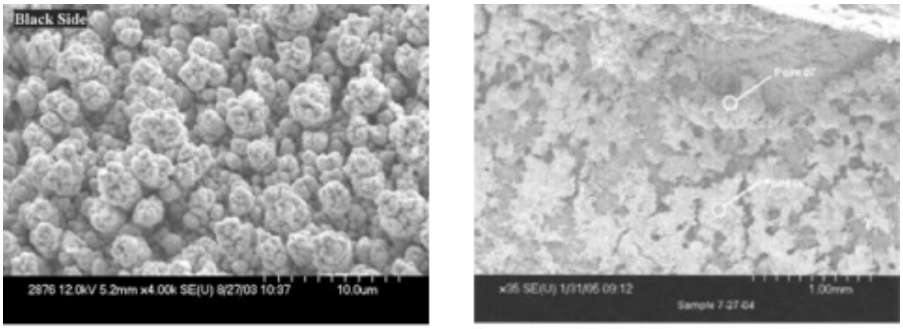

Figure 2. (a) SEM photograph of the electrode surface with no magnetic field applied. (b) Applied magnetic field.

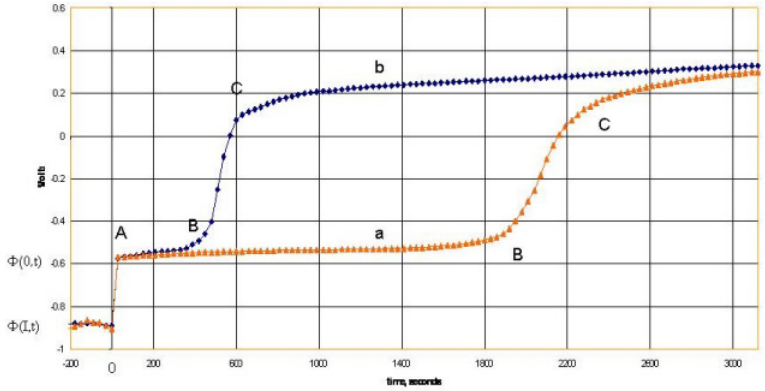

Figure 3. Hydrogen desorption rates. Curve a in the absence of magnetic field. Curve b in the presence of external magnetic field.

4. Experimental

4.1. Cell construction and operation

A rectangular cell, made of clear plastic, with affixed neutron detectors (CR-39 chips) and electrodes connected to a galvanostat (Princeton Applied Research, model 363) was placed in an external magnetostatic field. Upon placing an operating cell (with $i = -30$ mA cm^2) in the magnetic field, Fig. 4, electrochemical compression of absorbed hydrogen was put under computer controlled regime (LabView program) with $i = -400$ mA for 90 s and $i = 5.0$ mA for 5 s. The fabrication of cathodes involves (a) co-deposition from a solution of 0.03 M $PdCl_2$ and 0.3 M LiCl dissolved in H_2O at $i = -1.0$ mA/cm^2 for the first 24 h followed by $i = -3.0$ mA/cm^2 for the time required to reduce all the Pd^{2+} ions; (b) a 3–4 h stabilization period at $i = -30$ mA/cm^2, i.e. the time needed to assure uniform distribution of absorbed hydrogen throughout the electrode volume. Additional detail is provided by Szpak et al. [6].

4.2. The art of Pd + H co-deposition

The Pd + H co-deposition may be viewed as a special case of production of alloys by electrochemical processing. It involves simultaneous deposition of more than one component. This is done by the reduction of ions present in the electrolyte. Briefly, for the production of Pd/H alloy, the relevant reactions are: $Pd^{2+} + 2e^- \rightarrow Pd$ and $H_2O + e^- \rightarrow H + OH^-$. In practice, however, these reactions depend on the electrolyte composition. For the co-deposition from a solution containing $PdCl_4^{2-}$ complexes, Naohara [7] found that the reduction of Pd^{2+} proceeds via the reduction of an adsorbed $PdCl_4^{2-}$ complex resulting in a layer-by-layer growth of the Pd film. However, the orderly growth of deposited palladium is disturbed by the adsorbed hydrogen generated by the reduction of water. Ohmori et al. [8] using a scanning tunneling microscope, proposed a model where the H^+ ions are adsorbed and reduced at the surface. A part of the adsorbed hydrogen enters the Pd lattice and accumulates around lattice defects. Through this process, the surface is transformed into a modular-like structure. Figure 5 showing mechanism of growth and SEM of actual deposit.

Figure 6 illustrates the procedure when (i) reduction of $PdCl_4^{2-}$ and H_2O are independent of each other, (ii) electrolyte

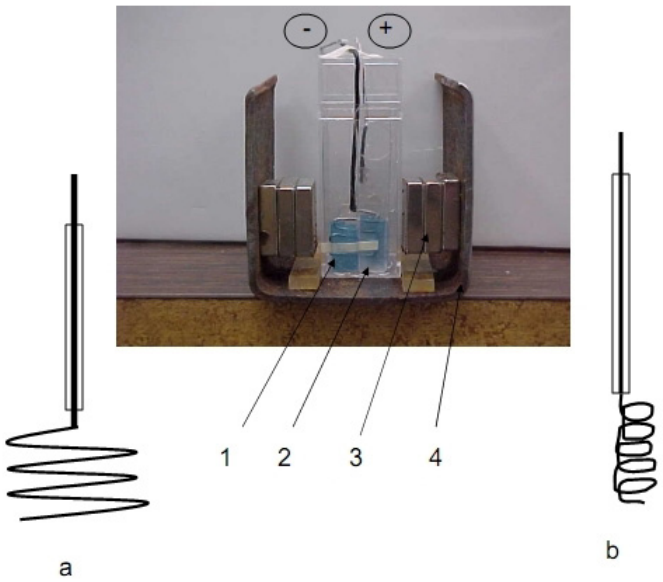

Figure 4. Electrochemical cell. 1–outside CR–39 detector, 2 – double CR–39 stock located inside the cell, 3 – neodymium magnets, 4 – magnet holder. Cathode and anode identified by Fig. 1a. Cathode assembly designed for neutron detection, 1 – CR–39 chips inside the cell, 2 – CR–29 outside the cell; Fig. 1b – for determination of deuterium content.

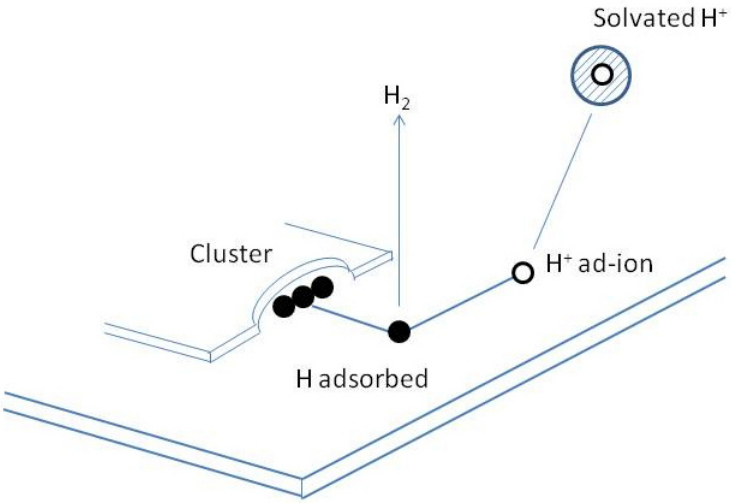

Figure 5. Representation of the development of micro-globules during co-deposition.

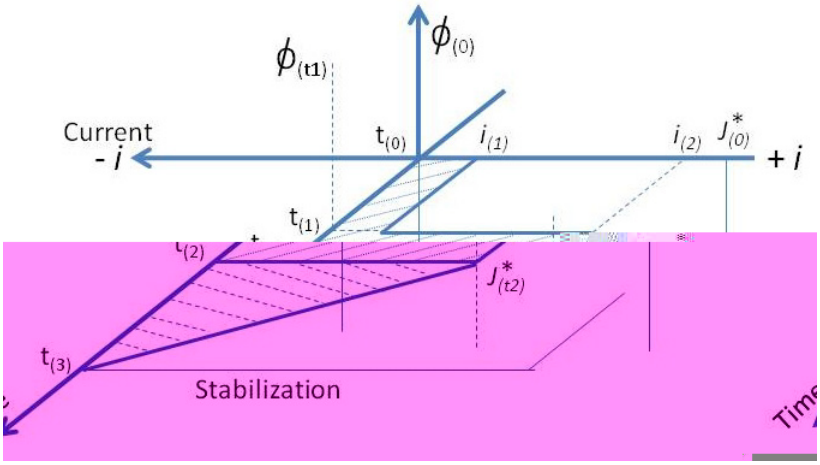

Figure 6. Cell current profile during the co-deposition process.

volume and electrode surface remain constant, (iii) reduction of Pd ions is diffusion controlled[a] and (iv) no other charge transfer reactions occur. Under these conditions the electrode rest potential, $\Phi(0)$, is determined by solution composition. At $t = 0$, a constant cell current, I_1, is applied. In practice it is much smaller than the limiting current, $I_1 \ll j_{1,\mathrm{lim}}$. Note that in Fig. 6, j^* denotes the limiting current. This is done to assure an adherent Pd deposit. With the passage of time, the Pd^{2+} ions are depleted, the electrode potential, driven by the cell current, becomes more negative. At $t = t_1$ the cell current is increased to I_2, i.e. to a value very close to the limiting current. This is done to assure a long co-deposition period. When the applied current density, I_2, by reducing the concentration of Pd^{2+} ions, becomes the limiting current (for that concentration), the electrode potential is driven into the region of heavy water instability and at $t = t_2$, the reduction of D^+ ions commences

5. Evidence

5.1. Detection of neutrons

Figure 7 shows typical images of tracks recorded on CR-39 chips. The examination of the CR-39 chips, located inside and outside, indicates no difference in the type of tracks but in their number, the latter being highest on the CR-39 detector facing the cathode and the lowest on the chip located outside the cell. In particular, Fig. 7(a) shows a typical distribution of images of circular and elliptical tracks, Fig. 7(b) and (c) illustrate the case of ionizing particle entering either perpendicular to the detector's surface or at an oblique angle, and Fig. 7(d) a double track. The physical meaning of the images recorded by CR-39 detectors is discussed in detail by Mosier–Boss et al. [9].

5.2. Deuterium detection

The mass spectrograph was used to analyze for deuterium. The Pd/H film co-deposited onto a thin coiled palladium wire was employed to assure retention of the electrochemically compressed hydrogen isotopes, Fig. 4(b). This electrode

[a]The diffusion limited current density is estimated by substituting $\delta = 0.05$ cm which yields $j^* = j_{\mathrm{lim}} = 0.025zc\ \mathrm{Acm}^{-2}$, where z is the number of positive charges and c in g-ion/l.

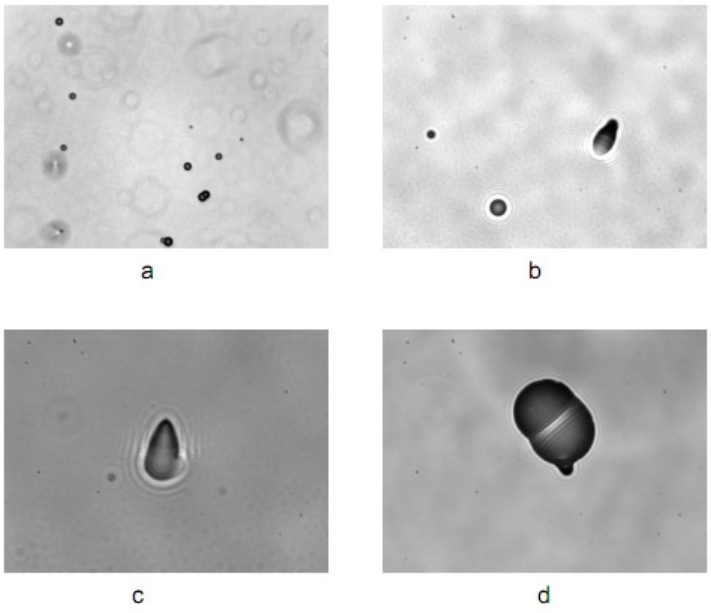

Figure 7. Images of tracks in CR-39 detectors created in the course of an experiment; a – distribution of tracks at 40×, b –illustrates the angle of impingement at 500×, c – shows a single track at 1000×, d – image of a double track at 500×.

design was selected to meet the requirements imposed by mass spectrograph. To minimize the desorption of hydrogen isotopes the following procedure was adapted (a) remove the cell from magnetostatic field, (b) stop the cell current flow, (c) take out the cathode, (d) cut-off the coiled part of the cathode and (e) analyze as soon as possible (e.g. within 15 min), utilizing the high vacuum of the mass spectrometer to greatly reduce the possibility that the hydrogen isotopes will form molecules as they diffuse out of the lattice.

The mass spectroscopic analysis, performed upon completion of a run, showed the presence of all hydrogen isotopes. Qualitatively, deuterium was the dominant isotope with negligible amounts of tritium. Typically, the D/H atomic ratio greater than one, with a value as high as 5:1, was recorded. Needless to say, that the presence of deuterium in the cathode is of utmost importance because it might provide decisive insight into the mechanism of nuclear reactions in condensed matter.

As a rule, mass spectroscopic analysis yields results that are unambiguous. However, if additional identification is required, then this can be done by (i) changing the method of analysis while retaining the sampling procedure or (ii) employing the original procedure (e.g. mass spectroscopy) and analyze after electrolysis of water with known D/H atomic ratios. Here, the latter was employed in which the desired D/H atomic ratios were obtained by electrolysis of a mixture of H_2O and D_2O in corresponding proportions using thin palladium wires as cathodes.

5.3. Catastrophic thermal events

Several catastrophic thermal events were observed (three out of ten). In one case, after three days of electrolysis with cell current varying between -300 mA cm^{-2} and 5 mA cm^{-2}, a catastrophic thermal event occurred that resulted in cell deformation, loss of electrolyte due to evaporation and leaking through a punctured cell bottom, Fig. 8.

Figure 8. Damaged cell bottom: a – outside view, b – inside view. Arrows indicate the well defined damage areas (1 – thinning, 2 – hole, 3 – embedded particles).

The damage, about 1/3 of total area, viewed from the outside, Fig. 8(a), and inside the cell, Fig. 8(b), is consistent with placing a very hot object in contact with plastic material. Examination of Fig. 8(a) of the cell damage, suggests that an explosive fragmentation of the Pd/H deposit occurred and a large segment hit the surface. The wall deformation implies that sufficiently high temperature softened the acrylic plastic. The intensity of the heat source can be estimated from the temperature raise of the electrolyte during the last 170 min of cell operation, Fig. 9.

Here, a cell, charged with 3.0 ml of 0.03 M $PdCl_2$ and maintained at a constant volume of 5.0 ml, was operated for two days before recording the solution temperature, with the thermocouple located below the cathode. Within the last 160 min the electrolyte temperature remained constant (at 50 C) followed by, at first, a slow raise for the next 4 min, section ABC, followed by a rapid increase, at 2.6 C/s, section DE. During the next 3–4 min, the electrolyte evaporated and the temperature returned to ambient. For this run, the intensity of the heat source, based on the heat generated by the minute amount of the PD/H film and transferred to the electrolyte, can be estimated to be more than 10 eV/Pd atom, i.e. outside the limits of chemical reaction. Moreover, the temperature raise of the source of ca 250 C/s means that substantial amount of the electrolyte was lost by “film boiling".

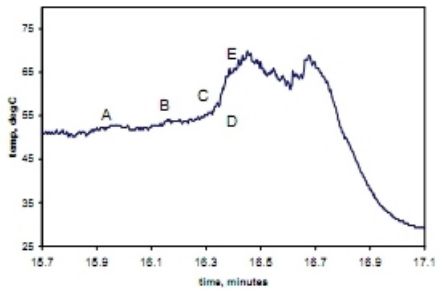

Figure 9. Temperature profile during thermal run-a-way.

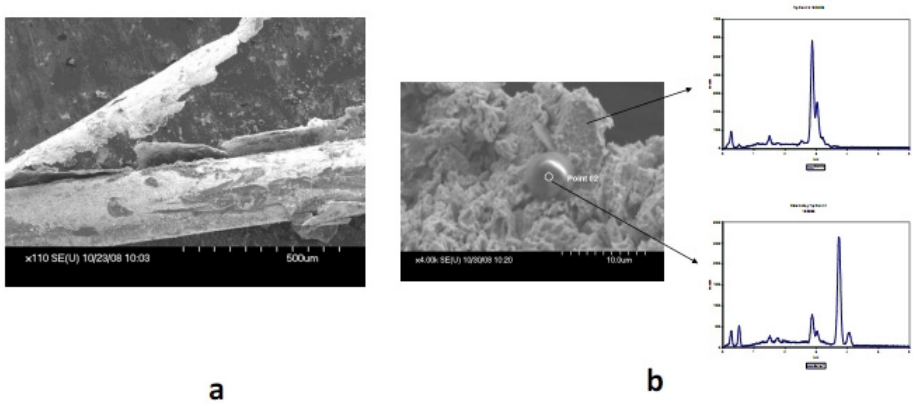

Figure 10. SEM/EDX SEM photograph illustrating separation of a Pd/H film during a mild run-a-way run. (a) – SEM photograph showing single reaction site; (c) – EDX of single reaction site (b) showing localized transmutation.

5.4. Mechanism of the Pd/H film separation

A probable, but speculative, mechanism of Pd/H film separation from the Pt substrate can be deduced using photograph, Fig. 10. The separation shown in Fig. 10 illustrates the separation of a Pd/D deposit in another set of experiments.

In particular, examination of Fig. 10(a) suggests the following: (i) a number of localized reactions at the Pt/Pd/D interface, indicated by an arrow, forced the separation of the Pd/D deposit from the Pt substrate, (ii) the SEM/EDX analysis of reaction sites contains participation of a nuclear event (transmutation) is involved in forcing film separation. The Pd/H film separation, shown in Fig. 8, occurred during a mild thermal run-a- way during electrolysis of light water is almost identical to that heavy water, thus suggesting the same mode of separation.

The film separation may be explosive. The damage, shown in Figs. 8a and (b), indicates that a Pd/H sleeve, after separation, was propelled away from the cathode and came in contact with the cell bottom. The high temperature and the amount of thermal energy necessary to generate the observed damage implies that thermal activity did not terminate upon separation from the cathode but persist during flight as well as after landing at the cell bottom.

6. Relevance

We have shown that chemical methodology is useful in studying conditions that initiate and maintain processes involving hydrogen and occurring within the confines of the palladium lattice. Here, we consider three cases: (i) the Widom–Larsen theory and experiment, (ii) reaction products and their usefulness and (iii) conceptual design of a power source.

6.1. The Widom–Larsen theory and experiment

Three facts that question the applicability of the Widom–Larsen theory to real systems, as applied to the polarized Pd/^{1}H–H_2O system, are considered. Those are: (i) the minimum value of heavy electrons, (ii) the ultra-low momentum neutrons and (iii) the location of the nuclear reactions.

6.1.1. *Heavy electrons*

Through the interpretation of the meaning of the reaction $e^- + p_l^+ \rightarrow n$ one can specify the necessary conditions for it to proceed, namely $\mu(n) - \mu(p_l^+) > 0$. Clearly, energies of both electron and proton must be considered. The energy

(heaviness) of the captured electron depends on the strength of p_l^+/Pd lattice defect interaction.

6.1.2. *Ultra-low momentum neutrons*

Qualitatively, viewing the electron capture as a chemical step, an addition of an electron (mass 0.91×10^{-27} g) to a proton (mass 1.66×10^{-24} g) does not substantially change the displacement velocity of the generated neutrons, i.e. neutron kinetic energy is that of the producing proton.

6.1.3. *Location of nuclear event*

Experimental evidence (specifically the emission of α^{2+} particles) shows that the nuclear event occurs within the interphase region. The exact location cannot be determined because it depends on the dynamics of the interphase region. Certainly, they do not occur at the contact surface which is occupied by hydrogen ad–ions subject to reduction to hydrogen atoms via the orbital capture of electrons. Incidentally, there is no known experimental method that would provide definite answer.

6.2. Reaction products and their usefulness

The sequence of events illustrated in Fig. 1 suggests some practical applications, arising from the kinetics of coupled reactions, e.g. (i) extraction of deuterium to increase D_2O/H_2O concentration in water, or as a neutron source and (ii) excess enthalpy production.

6.2.1. *Deuterium, and neutron extraction*

Both, deuterium and neutrons are the reaction products and both can be extracted. The specification of the correct procedure for maximum efficiency is dictated by the kinetics of coupled reactions (work currently in progress).

6.3. Excess enthalpy

Another, more interesting observation is that of excess enthalpy production. Returning to the temperature/time of Fig. 9, section BCD, the excess enthalpy is generated safely at high rates, i.e. just before the onset of the catastrophic event. Whether or not the high rate of excess enthalpy can be controlled cannot be determined before the reaction kinetics is known.

6.4. Conceptual design of power source

In principle, it is possible to design an electrochemical cell that utilizes the concept of power production. The set of reactions $e^- + p_l^+ \rightarrow n$, $e^- + d_l^+ \rightarrow 2n$ and $n + p_l^+ \rightarrow D^+$ forms the basis for a conceptual design of a power source. The co-deposited Pd/H film is the location of electrons and protons. If, within the film there is an added component, a substance, X, and if the $n + X \rightarrow X^* + Q$ reaction occurs, then it is possible to built a functioning device.

References

[1] S. Szpak, P.A. Mosier–Boss and J.J. Smith, *Phys. Let.* **A221** (1996) 141.
[2] S. Szpak, *J. Electroanal. Chem.* **373** (1994) 1.

[3] H. Remy, *Treatise on Inorganic Chemistry*, Vol. II, Elsevier, Amsterdam, 1956, p.563.
[4] L.D. Landau and E.M. Lifshitz, *Statistical Physics*, Vol. 5, part 1, Pergamon, Oxford, 1957, pp.318–319.
[5] R. Haase, *Thermodynamics of Irreversible Processes*, Adison-Wiley, London, 1969.
[6] S. Szpak, *J. Dea, J. Condensed Matter Nucl. Sci.* **9** (2012) 21.
[7] H. Naohara, S. Ye and K. Uosaki, *J. Phys. Chem B* **102** (1998) 4366.
[8] T. Ohmori, K. Sohamaki, K. Hashimoto and A. Fujishima, *Chemistry Letters*, The Chemical Society of Japan, 1991, p. 93.
[9] P.A. Moser-Boss, S. Szpak, F. Gordon and L.P.G. Forsley, *Naturwissenshaften* **96** (2005) 135.